Advanced Remote Sensing

http://publish.mersin.edu.tr/index.php/arsej

e-ISSN 2979-9104

Spatiotemporal prediction of reference evapotranspiration in Araban Region, Türkiye: A machine learning based approach

Ala Tahsin [1], Jazuli Abdullahi [2], Abdullah İzzeddin Karabulut [3], Mehmet İrfan Yesilnacar*[1]

[1]Harran University, Environmental Engineering Department, Sanliurfa, Türkiye ala.tahsin91@gmail.com, iyesilnacar@gmail.com
[2]Baze University, Center for Clean Energy and Climate Change, Plot 686 Cadastral Zone COO, Abuja, Nigeria, jazuli.abdullahi@bazeuniversity.edu.ng
[3]Harran University, Remote Sensing and Geographic Information Systems, Sanliurfa, Türkiye, karabulut6363@gmail.com

Cite this study: Tahsin, A., Abdullahi, J., Karabulut, A. İ., & Yeşilnacar, M. İ. (2023). Spatiotemporal prediction of reference evapotranspiration in Araban Region, Türkiye: A machine learning based approach. Advanced Remote Sensing, 3 (1), 27-37

Keywords
Meteorological variables
Artificial Neural Network
Evapotranspiration
Climate Change
Türkiye

Research Article
Received: 05.11.2022
Revised: 10.02.2023
Accepted: 12.03.2023
Published: 16.03.2023

Abstract

Accurate prediction of reference evapotranspiration (ET_0) is crucial for climate change mitigation, water resources management, and agricultural activities. Therefore, this study aimed at investigating the applicability of a recently developed machine learning model called Gaussian Process Regression (GPR), for the prediction of ET_0 in Araban station, Gaziantep region Türkiye. Artificial Neural Network was also developed for comparison. Several meteorological variables including temperatures T_{min}, T_{max} and T_{mean} (minimum, maximum and mean), surface pressure, wind speed and relative humidity from 1990 – 2021 were used as the inputs. The determination coefficient (R^2), root mean square error (RMSE), and mean absolute deviation (MAD) were used as performance evaluation criteria. The obtained results revealed that GPR led to better performance with MAD = 0.0174, RMSE (normalized) = 0.0236, and R^2 = 0.9940 in the validation step. The general results demonstrated that GPR could be employed successfully to accurately predict ET_0 in Araban station and thus, could be useful to decision makers and designers of water resources structures.

1. Introduction

Evapotranspiration (ET) plays a vital role in water resources management and planning and is amongst the most important components of hydrologic water cycle [1]. ET can be instrumentally measured or obtained by reference evapotranspiration (ET_0) calculation [2]. The ET_0 serve as the basis for computing crop evapotranspiration (ETc) as well as irrigation water requirement of crops [3]. Penman Monteith model by Food and Agricultural Organization of United Nations (FAO) has been accepted as the main method for estimating ET_0 in hourly, daily and monthly scales [4].

The history that relates ET to meteorological variables can be traced as back as early 19th century [5]. According to Chen et al. [6], up to six classes of methods have been developed including (1) mass transfer methods (for example, Shiri [7] improved mass transfer based ET_0 estimation approaches through wavelet-random forest methodology); (2) pan evaporation methods; (3) combination methods; (4) temperature based methods; (5) water budget methods and (6) radiation based methods (for example, Shiri [8] used mass transfer, temperature, radiation based ET_0 equations and a heuristic model to access the practical implications of ET_0 modeling in island environments.

For the past decades, artificial neural network (ANN) has been given significant attention in numerous fields of study including ET_0. Dimitriadou and Nikolakopoulos [9] applied for ET_0 prediction at Peloponnese Peninsula, Greece. Farooque et al. [10] employed ANN for daily ET_0 forecasting for sustainable irrigation scheduling. Under climate change scenarios, Maqsood et al. [11] projected ET_0 using ANN. Despite the nonlinearity of ANN and its ability to deal with nonlinear aspect of ET_0, it has some limitations which include over-fitting, time delay in choosing the best befitting structure etc. To overcome these and other issues, a recently developed model called Gaussian Process Regression (GPR) was employed in this study to predict ET_0 at Araban station, Gaziantep region in Türkiye.

2. Material and Method

2.1. Study Area

Araban is located in Gaziantep province of Türkiye and is bordered from North by Adıyaman district with latitudes (37°22° and 37°31). From South, Araban is bordered by Gaziantep district and Şanlıurfa left on its East side and Kahramanmaraş district on the West side. The climate of Araban is accepted as semi-arid region, Figure 1 shows the study area.

Figure 1. Study location in Türkiye

2.2. Data Normalization and Global Statistical Indicators

The data used in this study including temperatures T_{min}, T_{max} and T_{mean} (minimum, maximum and mean), surface pressure (P_S), wind speed (U_2) and relative humidity (R_H) from 1990 – 2021 were obtained from Türkiye meteorological organization and divided into 70% training (269) and 30% validation (115). Table 1 shows the descriptive statistics for all the data used. The independent variables used in this study were found to be influential for ET_0 modeling in several studies including Abdullahi et al. [12] and Abdullahi and Elkiran [13].

Table 1. Data descriptive statistics of the employed variables

Variable	Minimum	Maximum	Mean	St. Deviation	Kurtosis	Skewness
R_H (%)	22.0355	89.8997	55.2312	18.2547	−1.3730	−0.0860
P (mm/month)	0.0000	248.8500	37.8972	40.5243	3.5807	1.6687
T_{min} (^{0}C)	−6.5503	22.1477	8.6896	8.0374	−1.3313	0.0377
T_{max} (^{0}C)	2.9086	40.2871	21.7604	11.0927	−1.3727	0.0444
T_{mean} (^{0}C)	−2.0969	31.0013	14.9186	9.7376	−1.3688	0.0454
P_S (kpa)	90.6881	92.2619	91.5040	0.3559	−0.9030	−0.1344
U_2 (m/s)	1.6971	3.8572	2.4769	0.4224	−0.0557	0.7130

As seen in Table 1, the P values in the Araban region range between a minimum of 0 mm/month to a maximum of 248.850 mm/month which indicates that within the time span of the study, there were periods of dry season (no rainfall received) and periods of abundant rainfall (rainy season). The annual precipitation is above the threshold of water scarce climate (semiarid) which has amount between 200 – 700 mm/year according to Kašanin-Grubin et al. [14]. While the minimum and mean monthly temperatures (−6.5503 °C and −2.0969 °C) can be below the freezing point, the maximum temperature can be as high as 40 °C in the summer. As the percentage of water vapor is present in the air, the R_H can be as high as approximately 90% in Araban station.

The data used in this study were normalized to fall between 0 and 1 to ensure equal attention is given to all variables and to eliminate the inputs-output dimension according to Abdullahi and Tahsin [15] as:

$$D_n = \frac{D_i - D_{min}}{D_{max} - D_{min}} \tag{1}$$

Where D_i implies the ith data value and D_n, D_{max}, D_{min} represent the normalized, maximum and minimum data values, respectively.

Determination coefficient (R^2), root mean square error (RMSE) and mean absolute deviation (MAD) were used as performance indicator and information regarding them can be found from Ibrahim et al. [16] study as:

$$MAD = \frac{1}{N}\sum_{i=1}^{n} |p_i - a_i| \tag{2}$$

$$R^2 = 1 - \frac{\sum_{i=1}^{N}(a_i - p_i)^2}{\sum_{i=1}^{N}(a_i - \bar{a})^2} \tag{3}$$

$$RMSE = \sqrt{\frac{\sum_{i=1}^{N}(a_i - p_i)^2}{N}} \tag{4}$$

Where a_i, p_i, $\bar{a}$, and N are the actual values, predicted values, mean of the actual values, and number of observations, respectively.

2.3. Artificial neural network (ANN)

The neural network analysis process and artificial neural networks (ANN) have a set of features. Among them, most feed-forward ANN models have a multi-layered structure. The ANN's simple network design consists of three layers: input, hidden, and output [15-16]. The network receives the input data from the input layer, and the number of inputs depends on the number of nodes in this layer. The weights of each neuron are connected to those of the neurons in the opposite layer, and each neuron computes each input variable [17]. The most popular techniques for identifying the neurons and layers in hidden layers are trial and error methods [18]. The performance has a huge impact on improving the reliability of the study results [19]. ET0 and other climatic factors are effectively used for prediction by artificial technology. Many researchers have recently developed highly accurate discoveries and significant prediction data that will be based on observed data used for future planning and development. An artificial intelligence approach was used to analyze the data sets. The ANN has three layers,

as shown in Figure 2. The hidden input network serves as the intermediate input layer for all computations, while the output layer provides the final result for each input in the neural network [20].

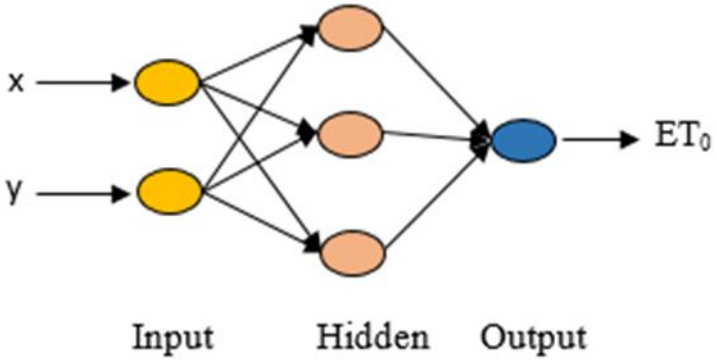

Figure 2. Artificial neural network structure [25]

2.4. Gaussian Process Regression (GPR)

A relatively new machine learning approach is the Gaussian process regression (GPR) model. Elbeltagi et al. [17] the two key characteristics of GPR are (1) the stochastic process explained by the multivariable Gaussian probability distribution (GPD), and (2) the unbiased forecasting based on the linear combination of prior experimental observation. The most mathematical aspects of the GPR for the inputs (Xi) and outputs (Yi) domains, where Xi and Yi are independently and identically distributed, are the covariance-based kernel function and mean function. The GPR is described as:

$$f(x) \sim GP\ (m(x), k(x,x)) \tag{5}$$

where $f(x)$ is the regression. For "y" observation, the Gaussian noise function is:

$$y = f(x) + \varepsilon \tag{6}$$

$$\varepsilon \approx N(0, \sigma_j^2) \tag{7}$$

Where ε represents the noise of normal distribution function with $N(0, \sigma_j^2)$. $k(x,x)$ described according to Akbari et al. (2019) [22] represent the new way for noise combination in covariance function given as follows:

$$k(x,x) = \sigma_j^2 \exp\left[\frac{-(x,x)^2}{2\tau^2}\right] + \sigma_n^2 \delta(x,x) \tag{8}$$

$\delta(x,x)$ is the Kronecker delta function, where n is the number of y observations. For processing inputs in high-dimensional feature space, selecting the right kernel can produce a decent map of the input series [23]. Below is a description of the key kernels. The Poly kernel, which enables the learning of nonlinear models, provides the similarity of vectors in a feature space.

$$k(x_i, x) = ((x_i, x) + 1)^d \tag{9}$$

The normalized kernel version can improve model building by reducing sparse data. It can be stated as:

$$k(x_i, x) = K(x_i, x) / \sqrt{K(x_i, x_i) K(x, x)} \tag{10}$$

A stationary kernel defined by the equation is called the radial basis function (RBF), often known as the "squared exponential" (11).

$$k(x_i, x) = e^{-\gamma |x_i - x|^2} \tag{11}$$

The Pearson Universal Kernel (PUK), an alternative to the general kernel function for curve fitting, was proposed by Pearson (1895). As shown in Equation 12, the kernel is mathematically described:

$$k(x_i, x) = (1/[1 + (2\sqrt{\| x_i - x \|}^2 \sqrt{2^{(\frac{1}{\omega})} - 1/\sigma)^2}]^{\omega} \quad (12)$$

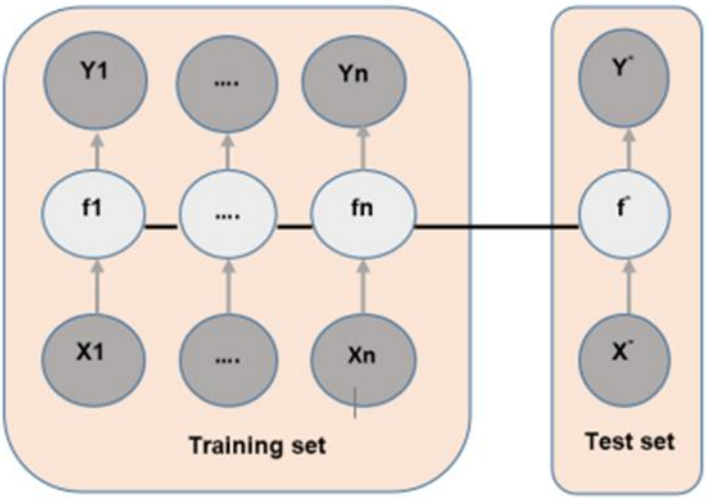

Figure 3. Probabilistic graphical model or functioning of Gaussian process regression [21]

2.5. Reference evapotranspiration (ET_0)

According to Allen et al. [4], for estimating ET_0 the most common used energy balance physical-based equation is the Penman-Monteith equation (FAO56-PM) as proposed by the Food and Agriculture Organization (FAO). The (FAO56-PM) equation's performance is widely acknowledged as the most expert equation for estimating ET_0 [24]. The equation is given by Allen et al. [4] and Abdullahi et al. [25]:

$$ET_0 = \frac{0.408\Delta(R_n - G) + \gamma \frac{900}{T + 273} U_2(e_s - e_a)}{\Delta + \gamma(1 + 0.34U_2)} \quad (13)$$

Where $\boldsymbol{ET_0}$ is the reference evapotranspiration (mm/day), Δ is slope vapor pressure curve (kpa/°C), $\boldsymbol{R_n}$ is net radiation at the crop surface (MJ/m²/day), G is soil heat flux density (MJ/m²/day), T is air temperature at 2 m height (°C), $\boldsymbol{U_2}$ is wind speed at 2 m height (m/s), $\boldsymbol{e_s}$ is saturation vapor pressure (kpa), $\boldsymbol{e_a}$ is actual vapor pressure (kpa), $\boldsymbol{e_s - e_a}$ is saturation vapour pressure deficit (kpa), γ is psychrometric constant (kpa/°C).

3. Results and Discussion

In this study, the recently developed GPR model was applied to predict ET_0 and compared with ANN model. Hence, the results are presented accordingly. Determining the dominant inputs can play a crucial role in modeling and prediction of ET_0. Therefore, correlation analysis was performed to ascertain the most appropriate input variables in this study. Table 2 presents the correlation matrix of the employed variables.

Table 2. Correlation analysis results of the used variables

	T_{min}	R_H	P	T_{mean}	T_{max}	P_S	U_2	ET_0
T_{min}	1							
R_H	−0.9138	1						
P	−0.6529	0.7619	1					
T_{mean}	0.9966	−0.9258	−0.6778	1				
T_{max}	0.9921	−0.9401	−0.7028	0.9984	1			
P_S	−0.7642	0.6432	0.4191	−0.7869	−0.7807	1		
U_2	0.6307	−0.6577	−0.4622	0.6642	0.6763	−0.7881	1	
ET_0	0.9432	−0.9139	−0.6827	0.9605	0.9649	−0.8563	0.8173	1

As shown by Table 2, due to the significance of temperatures, T_{max}, T_{mean}, and T_{min} in descending order are more correlated with ET_0 than other variables with 0.9649, 0.9605, and 0.9432, respectively. In other words, temperature variables are the factors with the most influence on the ET_0 prediction at Araban station. With this, it can be said that including the temperature variables as inputs would have a profound effect on the prediction skills of the machine learning (ML) models. The correlation of the input variables in descending order is T_{max}, T_{mean}, T_{min}

in, U_2, P, P_S, and R_H. However, for ML applications, apart from the dominant variables, the input size has a great role to play in determining the highest performance. Therefore, 2 different input combinations were developed given as:

$$M1 = f(R_H, P, T_{mean}, T_{max}) \quad (14)$$

$$M2 = f(T_{min}, Ps, U_2) \quad (15)$$

It is worthy to clarify that these two input combinations of the models were selected due to the relation between the ET_0 and the independent variables as demonstrated by Table 2. However, this study tried to ascertain the influence of number of inputs with respect to the ET_0 prediction. As such, rich (4) and limited (3) input combinations were considered as shown by Equations (14) and (15).

Where M1 and M2 are the developed models for ET_0 prediction. The results of the ET_0 prediction are shown in Table 3.

Table 3. Results of the predicted ET_0 based on ANN and GPR

		Training			Validation		
Model type	Model N0.	MAD	RMSE	R2	MAD	RMSE	R2
ANN	M1	0.0286	0.0401	0.9813	0.0299	0.0412	0.9816
	M2	0.0308	0.0383	0.9841	0.0294	0.0380	0.9832
GPR	M1	0.0173	0.0224	0.9941	0.0174	0.0236	0.9940
	M2	0.0241	0.0311	0.9888	0.0244	0.0323	0.9887

As seen in Table 3, using different input combinations, different performances are achieved for both ANN and GPR models. For ANN models, similar performances are obtained. Although there is a slight difference between the developed models in the training step, the results are comparable in the validation step with R2 values of 0.9816 and 0.9832 for M1 and M2, respectively. This shows that the accurate prediction of ET_0 by ML does not depend on the number of inputs used, but rather on the quality of inputs. As such, M2 with 3 inputs can appropriately predict the behavior of the ET_0 with less computational difficulties and less time-consuming. The improved performance of M2 could be attributed to the inclusion of U2 as input. According to Nourani et al. [18], despite having less influence on ET_0 prediction when single input single output prediction is considered, U2 significantly improves performance when combined with other variables as ET_0 inputs. Figure 4 shows scatter plots and histograms of the observed and predicted ET_0 for the best model (M2).

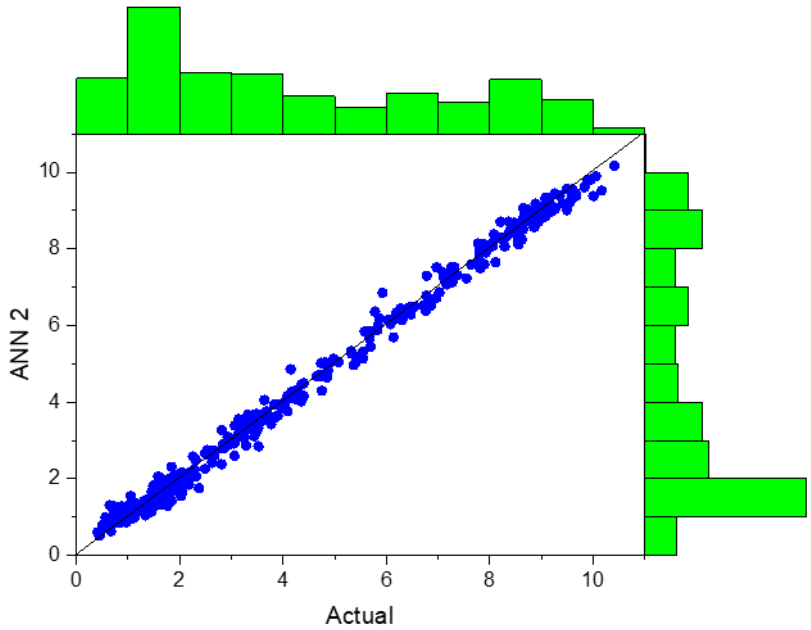

Figure 4. Graphical comparison of the observed and predicted ET_0 values for the best model

As can be seen in Figure 4, both actual and predicted values are concentrated towards the bisector line (line 1:1) which implies an agreement between prediction by ANN2 and the actual ET_0. It can also be seen with respect to the histogram in Figure 4 that the predicted values resemble the actual values.

It is obvious from Table 3 contrary to the results for ANN models where M2 surpasses M1, the results for GPR models show an improved performance of M1 over M2 by 0.53%. The reported performances based on MAD, RMSE and R^2 for M1 are 0.0173, 0.0224 and 0.9941 in the training step and 0.0174, 0.0236 and 0.9940 in the validation step. Whereas for M2, the MAD, RMSE and R^2 values are 0.0241, 0.0311 and 0.9888 in the training step and 0.0244, 0.0323 and 0.9887 in the validation step. Figure 5 shows the scatter plots and histogram of the actual and GPR M1.

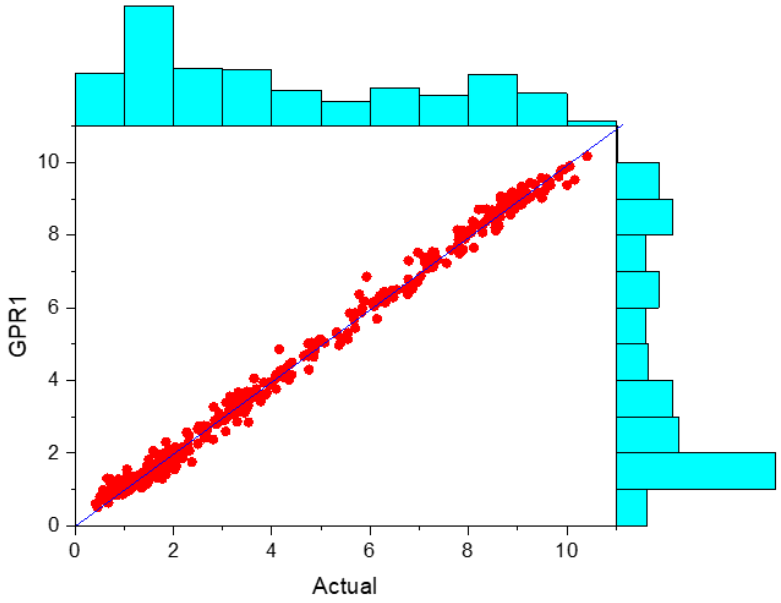

Figure 5: comparison of actual values and best GPR model

As shown by Figure 5, there is a good agreement between the actual and predicted values by GPR1. This shows that when adequate prediction skills are achieved, both the numerical and graphical results will exhibit similar outcomes. In terms of the histogram, the comparison shows how fitted values of the GPR1 model with respect to actual values. Besides the goodness of fit of the predicted values with respect to the actual values, graphical comparison in terms of error generated would be helpful in ascertaining the performance of the developed models. As such, Figure 6 demonstrates the performances of all the developed models based on MAD and RMSE.

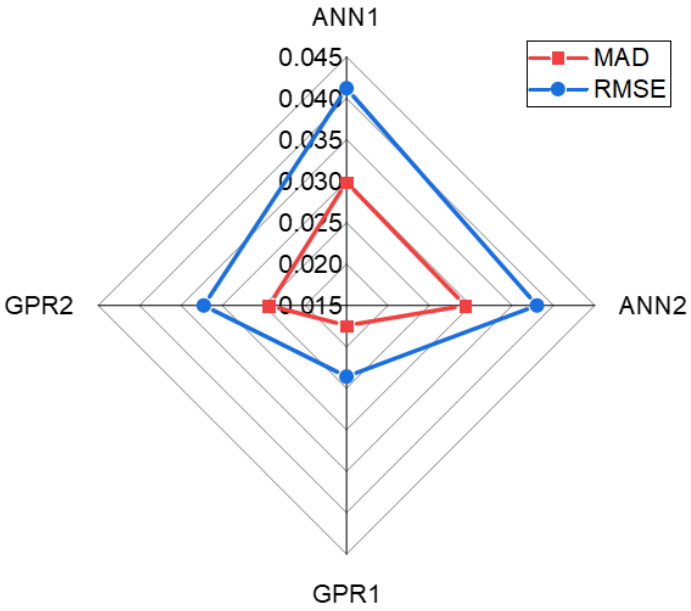

Figure 6. Performance comparison of all the developed models

Figure 6 compares the performance of all the applied models ANN1, ANN2, GPR1 and GPR2. It can be deduced from the figure that all the models could successfully be employed for ET_0 prediction at Araban station with a minimal error. The employed radar chart indicates better performance with narrower value and less efficiency is achieved with wider value. Owing to this, it can be observed that with respect to the ML models developed, GPR led to better accuracy. In the meantime, GPR1 was found to be the most efficient performance when both MAD and RMSE are considered.

However, to ensure robust assessment of the developed models, other performance metrics were applied via Taylor diagrams. The overall model performances are summarized using Taylor diagrams by taking into cognizance the RMSE between the model predictions and observed data, as well as pattern correlation and variability [26]. Standard deviation (SD), RMSE and correlation coefficient (CC) in the diagram are used to assess the similarity between predicted and observed records. Generally, underestimation is said to have occurred when the SD of the predicted values is lower than the SD of the actual values. Contrarily, overestimation occurs when the SD of the predicted values surpasses the SD of the actual values [27]. Figures 7 and 8 show the Taylor diagrams of the applied models in the training and validation steps.

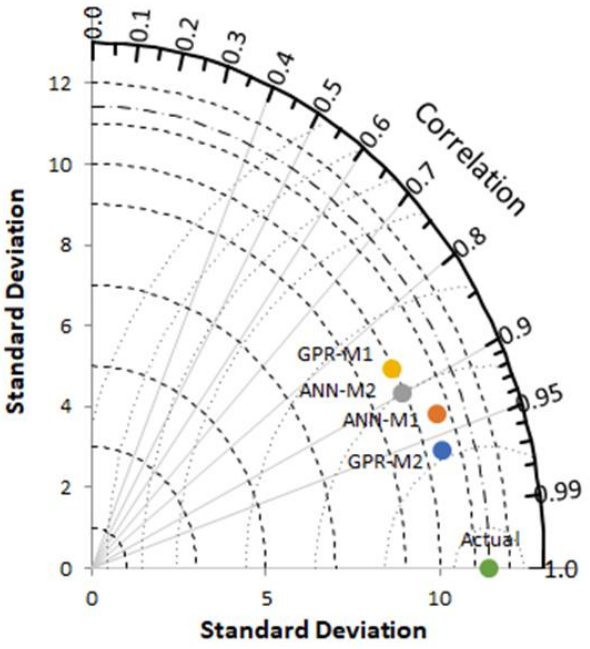

Figure 7. Performance comparison based on the Taylor diagram in the training step

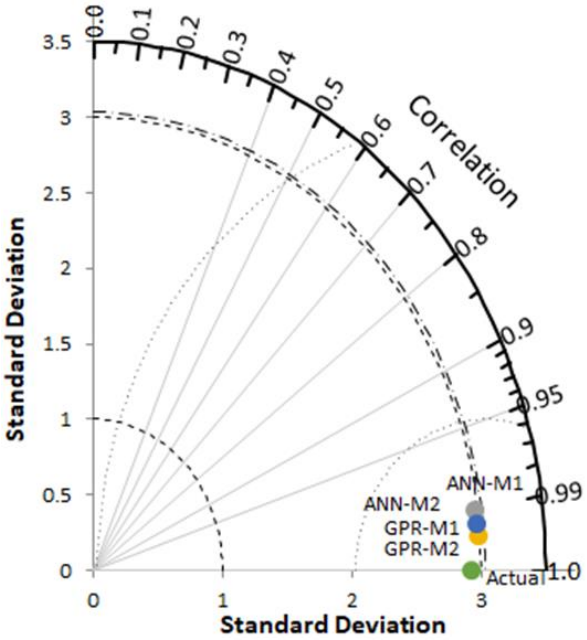

Figure 8. Performance comparison based on the Taylor diagram in the validation step

As can be observed in the Taylor diagrams, different performances are displayed by different indices considered. In the validation step (Figure 8), all the models have SD values close to the actual value. In terms of CC, GPR-M2 demonstrated more efficient performance but all the models have CC values above 0.99.

Intensification of agricultural activities through reduction of environmental impacts and increase in production with respect to plants per unit area is the best approach to ensure food production increase in a more sustainable manner (Farias et al. [30]). The increase in agricultural activities in Araban will in turn increase irrigation practice in the region.

Furthermore, improvement in irrigation practices may lead to conflicts over water use especially in areas where water is scarce. Therefore, accurate prediction of water losses is essential in agricultural and irrigation practices in Araban region. In such circumstances, strategies for irrigation management can essentially be developed through the precise estimation of crop evapotranspiration (ETc). According to Elkiran and Abdullahi [31] study, the ETc is obtained by multiplying crop coefficient (Kc) with ET_0. Consequently, accurate prediction of ET_0 achieved in this study will assist in ascertaining the ETc in the area which will in turn help in improving the agricultural water management and irrigation practices in Araban region.

4. Conclusion

This study was performed to assess the possibility of employing a recently developed model called gaussian process regression (GPR) to improve the performance of machine learning (ML) based artificial neural network (ANN) for the spatiotemporal prediction of reference evapotranspiration (ET_0) in Araban, Gaziantep region, Türkiye. To achieve this, 2 different input combination models were developed using R_H, P, T_{mean}, and T_{max} as M1 and T_{min}, P_S, and U_2 as M2 for both ANN and GPR models for data that spanned from 1990 - 2021.

The obtained results showed that the ML models are sophisticated tools for ascertaining the stochastic phenomena surrounding ET_0. Both M1 and M2 can lead to high performance but M2 slightly outperforms M1. However, when fewer simulation difficulties, as well as less time-consuming, are more important, M1 is preferable. The overall results show that GPR performance is better than ANN. From the results of this study, it is obvious that GPR model with its high precision can be applied in several regions in Türkiye in particular and world at large for the prediction of ET0. For regions that share similar meteorological climate, for instance Gaziantep district, similar results can be achieved and the results from the Araban station can be extended other locations within the vicinity of the climate.

Acknowledgement

This study was partly presented at the 5th Intercontinental Geoinformation Days [32].

Funding

This research received no external funding.

Author contributions

Jazuli Abdullahi: Conceptualization, Methodology, Software **Ala Tahsin:** Data curation, Writing-Original draft preparation, Software, Validation. **Mehmet Irfan Yesilnacar:** Visualization, Investigation, Writing-Reviewing and Editing. **Abdullah İzzeddin Karabulut:** Visualization, Map Creation, Writing-Reviewing and Editing.

Conflicts of interest

The authors declare no conflicts of interest.

References

1. Abdullahi, J., Elkiran, G., & Nourani, V. (2017). Application of artificial neural network to predict reference evapotranspiration in Famagusta, North Cyprus. In 11th International Scientific Conference on Production Engineering Development and Modernization of Production (pp. 549-554).
2. Gocić, M., Motamedi, S., Shamshirband, S., Petković, D., Ch, S., Hashim, R., & Arif, M. (2015). Soft computing approaches for forecasting reference evapotranspiration. Computers and Electronics in Agriculture, 113, 164-173.
3. Dai, X., Shi, H., Li, Y., Ouyang, Z., & Huo, Z. (2009). Artificial neural network models for estimating regional reference evapotranspiration based on climate factors. Hydrological Processes: An International Journal, 23(3), 442-450.
4. Allen, R. G., Pereira, L. S., Raes, D., & Smith, M. (1998). Crop evapotranspiration-Guidelines for computing crop water requirements-FAO Irrigation and drainage paper 56. *Fao, Rome*, *300*(9), D05109.
5. Nourani, V., Elkiran, G., & Abdullahi, J. (2020). Multi-step ahead modeling of reference evapotranspiration using a multi-model approach. Journal of Hydrology, 581, 124434.
6. Chen, D., Gao, G., Xu, C. Y., Guo, J., & Ren, G. (2005). Comparison of the Thornthwaite method and pan data with the standard Penman-Monteith estimates of reference evapotranspiration in China. Climate research, 28(2), 123-132.
7. Shiri, J. (2018). Improving the performance of the mass transfer-based reference evapotranspiration estimation approaches through a coupled wavelet-random forest methodology. Journal of Hydrology, 561, 737-750.
8. Shiri, J. (2019). Modeling reference evapotranspiration in island environments: assessing the practical implications. Journal of Hydrology, 570, 265-280.
9. Dimitriadou, S., & Nikolakopoulos, K. G. (2022). Artificial neural networks for the prediction of the reference evapotranspiration of the Peloponnese Peninsula, Greece. Water, 14(13), 2027.

10. Farooque, A. A., Afzaal, H., Abbas, F., Bos, M., Maqsood, J., Wang, X., & Hussain, N. (2022). Forecasting daily evapotranspiration using artificial neural networks for sustainable irrigation scheduling. Irrigation Science, 40(1), 55-69.
11. Maqsood, J., Farooque, A. A., Abbas, F., Esau, T., Wang, X., Acharya, B., & Afzaal, H. (2022). Application of artificial neural networks to project reference evapotranspiration under climate change scenarios. Water Resources Management, 36(3), 835-851.
12. Abdullahi, J., Elkiran, G., Malami, S. I., Rotimi, A., Haruna, S. I., & Abba, S. I. (2021, July). Compatibility of Hybrid Neuro-Fuzzy Model to Predict Reference Evapotranspiration in Distinct Climate Stations. In 2021 1st International Conference on Multidisciplinary Engineering and Applied Science (ICMEAS) (pp. 1-6). IEEE.
13. Abdullahi, J., & Elkiran, G. (2022). Monthly prediction of reference evapotranspiration in northcentral Nigeria using artificial intelligence tools: a comparative study. In 11th International Conference on Theory and Application of Soft Computing, Computing with Words and Perceptions and Artificial Intelligence-ICSCCW-2021 11 (pp. 165-172). Springer International Publishing.
14. Kašanin-Grubin, M., Vergari, F., Troiani, F., & Della Seta, M. (2018). The role of lithology: Parent material controls on badland development. In Badlands dynamics in a context of global change (pp. 61-109). Elsevier.
15. Abdullahi, J. and Tahsin, A. (2020). Data-Driven Techniques for Monthly Pan Evaporation Modeling in Iraq. Eurasian Journal of Science & Engineering, 6(1), 104-120.
16. Ibrahim, Z., Tulay, P., & Abdullahi, J. (2022). Multi-region machine learning-based novel ensemble approaches for predicting COVID-19 pandemic in Africa. Environmental Science and Pollution Research, 1-23.
17. Elbeltagi, A., Kushwaha, N. L., Rajput, J., Vishwakarma, D. K., Kulimushi, L. C., Kumar, M., ... & Abd-Elaty, I. (2022a). Modelling daily reference evapotranspiration based on stacking hybridization of ANN with meta-heuristic algorithms under diverse agro-climatic conditions. Stochastic Environmental Research and Risk Assessment, 1-24.
18. Kumar, N., Adeloye, A. J., Shankar, V., & Rustum, R. (2020). Neural computing modelling of the crop water stress index. Agricultural Water Management, 239, 106259.
19. Abyaneh, HZ., Bayat Varkeshi, M., Golmohammadi, G., & Mohammadi, K. (2016). Soil temperature estimation using an artificial neural network and co-active neuro-fuzzy inference system in two different climates. Arabian Journal of Geosciences, 9(5), 1-10.
20. Bajirao, T. S., Kumar, P., Kumar, M., Elbeltagi, A., & Kuriqi, A. (2021). Superiority of hybrid soft computing models in daily suspended sediment estimation in highly dynamic rivers. Sustainability, 13(2), 542.
21. Abrishami, N., Sepaskhah, A. R., & Shahrokhnia, M. H. (2019). Estimating wheat and maize daily evapotranspiration using artificial neural network. Theoretical and Applied Climatology, 135(3), 945-958.
22. Malik, A., Tikhamarine, Y., Al-Ansari, N., Shahid, S., Sekhon, H. S., Pal, R. K., ... & Sammen, S. S. (2021). Daily pan-evaporation estimation in different agro-climatic zones using novel hybrid support vector regression optimized by Salp swarm algorithm in conjunction with gamma test. Engineering Applications of Computational Fluid Mechanics, 15(1), 1075-1094.
23. Elbeltagi, A., Salam, R., Pal, S. C., Zerouali, B., Shahid, S., Mallick, J, & Islam, A. R. M. (2022b). Groundwater level estimation in northern region of Bangladesh using hybrid locally weighted linear regression and Gaussian process regression modeling. Theoretical and Applied Climatology, 1-21.
24. Akbari, M., Salmasi, F., Arvanaghi, H., Karbasi, M., & Farsadizadeh, D. (2019). Application of Gaussian process regression model to predict discharge coefficient of Gated Piano Key Weir. Water Resources Management, 33(11), 3929-3947.
25. Kumar, M., Tiwari, N. K., & Ranjan, S. (2019). Kernel function based regression approaches for estimating the oxygen transfer performance of plunging hollow jet aerator. Journal of Achievements in Materials and Manufacturing Engineering, 95(2).
26. Sobh, M. T., Nashwan, M. S., & Amer, N. (2022). High Resolution Reference Evapotranspiration for Arid Egypt: comparative analysis and evaluation of empirical and artificial intelligence models. International Journal of Climatology.
27. Abdullahi, J., Elkiran, G., & Nourani, V. (2019a). Artificial intelligence based and linear conventional techniques for reference evapotranspiration modeling. In International Conference on Theory and Application of Soft Computing, Computing with Words and Perceptions (pp. 197-204). Springer, Cham.
28. Abdullahi, J., Iravanian, A., Nourani, V., & Elkiran, G. (2019b). Application of artificial intelligence based and multiple regression techniques for monthly precipitation modeling in coastal and inland stations. Desalin. Water Treat., 177, 338-349.
29. Elkiran, G., Nourani, V., & Abba, S. I. (2019). Multi-step ahead modelling of river water quality parameters using ensemble artificial intelligence-based approach. Journal of Hydrology, 577, 123962.
30. Dos Santos Farias, D. B., Althoff, D., Rodrigues, L. N., & Filgueiras, R. (2020). Performance evaluation of numerical and machine learning methods in estimating reference evapotranspiration in a Brazilian agricultural frontier. Theoretical and Applied Climatology, 142, 1481-1492.

31. Elkiran, G., & Abdullahi, J. (2019). Assessment of water balance in food trade in the water-scarce regions of Nigeria. International Transaction Journal of Engineering, Management, & Applied Sciences & Technologies, 10(3), 299-308.
32. Yesilnacar M, I., Tahsin J. A, & Karabulut A. I. (2022). Spatiotemporal prediction of reference evapotranspiration in Araban region, Turkey: A machine learning based approaches. Intercontinental Geoinformation Days (IGD), 5, Netra, India